A Critical Comparison of Approximation Methods and Models for Equilibrium Properties of Low-Barrier Hydrogen Bonds

David A. MacDonald, Gregory E. Eppard, Christopher J. Halkides, and Michael Messina*

Department of Chemistry, University of North Carolina at Wilmington, Wilmington, North Carolina 28403

Received July 29, 2002

Recent experimental evidence has led to the conclusion that short, strong hydrogen bonds can stabilize transition states of enzyme catalyzed biochemical reactions. Evidence for such hydrogen bonds is the low value of the isotopic fractionation factor, ϕ, which is defined as the equilibrium constant for the generic reaction, R−H + DOH ↔ R−D + HOH, where H is the hydrogen atom participating in the low-barrier hydrogen bond in a molecule R−H. In this work we assess two approximation methods for computing the isotopic fractionation factors for single and multidimensional systems containing a low-barrier hydrogen bond. These methods are WKB and an approach that corrects the classical partition function via a quantum correction factor. We find that the latter approach is universally accurate and applicable in both single and multidimensional systems containing a low-barrier hydrogen bond. We also assess two different models for the coupling of a molecule's low-barrier hydrogen bond to other degrees of freedom, both internal and external to the molecule, and show that each leads to a lowering of the fractionation factor.

I. INTRODUCTION

Low-barrier hydrogen bonds (LBHB) between enzyme−substrate complexes are believed to be an important kinetic step in enzyme catalyzed biochemical reactions.[1−10] An important, recent example, is the experimental evidence that has led to the conclusion that short, strong hydrogen bonds can stabilize transition states of enzyme catalyzed biochemical reactions.[1−7] Evidence for such hydrogen bonds is the low value of the isotopic fractionation factor, ϕ, which is defined as the equilibrium constant for the generic reaction, ES−H + DOH ↔ ES-D + HOH. (H is the hydrogen atom participating in the LBHB in an enzyme−substrate complex, ES.) For example, low fractionation factors were measured for enzyme groups involved in acid−base catalysis of pyruvate and biotin carboxylases. A low ϕ value is attributed to the formation of a LBHB. In any intramolecular hydrogen bond, the H atom is covalently bound to a donor site and hydrogen bonded to an acceptor site. In the LBHB, the energetic barrier between the donor and acceptor sites is low, and the distance between the donor and acceptor sites is small (typically, below 250 pm). Hence, the LBHB has important thermodynamic (the energetic barrier) and structural (donor−acceptor distance) impact on enzyme transition states. Experimental results described in the literature provide strong evidence for intermolecular LBHBs, in which the proton is shared between donor and acceptor sites on different molecules. In this paper, we will focus on intramolecular LBHBs, where the proton is shared between donor and acceptor sites in the same molecule. We focus on intramolecular LBHBs because they are easier to handle computationally, and there is more experimental evidence available with which to compare theoretical results.

* Corresponding author phone: (910)962-7298; e-mail: messinam@uncwil.edu.

Kreevoy and Liang were the first to propose an explanation for the correlation between small ϕ values and LBHBs.[11] They treated the important proton coordinate involved in the LBHB as a single-dimensional double well potential. Kreevoy and Liang then computed fractionation factors for several different double well potentials and found that low fractionation factors arose when the barrier between the donor and acceptor sites was low energy.

Unfortunately, an intramolecular-molecular hydrogen bond does not exist alone. The proton must be coupled to both intramolecular vibrations and the external solvent degrees of freedom. It is well-known that exact computation of quantum partition functions for such multitudinous systems becomes computationally prohibitive. Further, the exact solutions to such a problem are so complicated that they do not lead to a physically intuitive picture of the effect of other modes of motion on the LBHB.

In this work we compare the accuracy of two different approximation methods for computing the quantum partition function of a LBHB. One approach, WKB,[12] is limited to application to the single-dimensional picture of the LBHB. The advantage of this method is that it leads to an analytical expression for the fractionation factor that can be computed on a hand calculator. The second approximation scheme involves computing the quantum partition function by applying a simple correction term to the classical partition function.[13] We term this method the quantum correction method (QCM). The advantages of the QCM are that it is applicable to multidimensional systems and leads to a physically intuitive picture of the effects of external degrees of freedom on the equilibrium properties of the LBHB. The disadvantage of this approach is that it relies on numerical integration that must be performed computationally and, thus, does not lead to an analytic expression for the fractionation factor. This disadvantage is not too hard to bear since we

10.1021/ci0202943 CCC: $22.00
Published on Web 10/25/2002

will show that the computations involved in this approximation, even for a system as large as 20−30 degrees of freedom, can be performed extremely accurately and efficiently. Once we demonstrate the efficiency and accuracy of the QCM we apply it to two different, but physically reasonable models, for coupling of the intramolecular LBHB to other degrees of freedom. The first model couples the LBHB coordinate directly to an intramolecular vibrational mode that modulates the barrier height. This model captures the effect of a vibration that modulates the distance between the donor and acceptor sites, thus modulating the barrier height. The second model couples the LBHB coordinate to a set of harmonic oscillators that mimics the effect of an external solvent on the LBHB. We will show that both models have the effect of *lowering* the isotopic fractionation factors from those of the analogous single-dimensional system.

This paper is organized as follows. In Section II (a) we present the set of equations needed to compute the quantum partition functions and fractionation factors within the QCM and WKB approximations. In Section II (b) we define and discuss the two multidimensional models for the coupling of the intramolecular LBHB to other degrees of freedom. In Section III (a) we present numerical results that assess the accuracy of the QCM and WKB approximations for computation of quantum partition functions and fractionation factors in a single-dimensional system by comparing to exact results. In Section III (b) we present numerical results obtained from the QCM approach of isotopic fractionation factors for our two models that couple the LBHB to other degrees of freedom.

II. THEORY

(a) Approximation Methods. Here we derive the equations required for the two approximate approaches to computing the quantum partition functions and fractionation factors of a LBHB. The model potential for the proton involved in the LBHB is that of a double well. We have shown in previous work that a quadratic-quartic potential suffices for representing the proton coordinate[14]

$$V(x) = Ax^4 - Bx^2 + D \tag{1}$$

The coordinate x measures the distance of the proton from the donor site, while the constants A and B set the curvature at the well minima and the barrier height. The barrier height is given by, D

$$D = \frac{B^2}{4A} \tag{2}$$

The distance between the minima, Δx, and the curvature at the well minima, k, are given by

$$\Delta x = \sqrt{\frac{2B}{A}} \tag{3a}$$

$$k = 4B \tag{3b}$$

This double well potential is shown in Figure 1. As is well-known, the double well potential has a manifold of doublet eigenstates below the barrier which coalesce into singlet eigenstates above the barrier. Shown within Figure 1 are the first three eigenvalues of this potential when the barrier height is 16.5 kJ mol^{-1}.

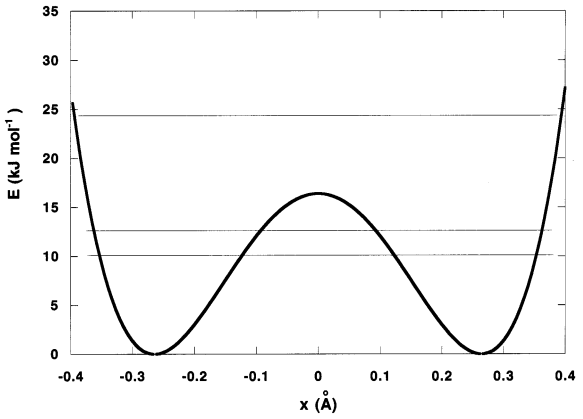

Figure 1. Double well potential, for a barrier height 16.5 kJ mol^{-1}, showing the values of the first three eigenenergies.

The quantum mechanical partition function, Q, can be computed exactly by the Boltzmann sum over all the eigenstates, E_J

$$Q = \sum_J e^{-\beta E_J} \tag{4}$$

where β is the inverse temperature ($1/kT$). (k is the Boltzmann constant and T is the temperature.)

Once the quantum mechanical partition function is known then any equilibrium property of the system can be computed. Of particular interest in the case of a LBHB is the fractionation factor, ϕ, the equilibrium constant for the generic reaction

$$R - H + DOH \leftrightarrow R - D + HOH \tag{5}$$

The fractionation factor can thus be written in terms of reactant and product concentrations as

$$\phi = \frac{[R - D][H - OH]}{[R - H][D - OH]} \tag{6}$$

The fractionation factor can also be written as the following ratio of partition functions for reactants and products[15]

$$\phi = \left(\frac{Q_{R-D}}{Q_{R-H}}\right)\left(\frac{Q_{H-OH}}{Q_{D-OH}}\right) \tag{7}$$

Since the ratio of protonated and deuterated water partition functions are the same and independent of the molecule containing LBHB, we focus on the reduced fractionation factor given below

$$\phi_R = \left(\frac{Q_{R-D}}{Q_{R-H}}\right) \tag{8}$$

The reduced fractionation factor, ϕ_R, can thus be computed from the quantum mechanical partition function of the protonated and deuterated species.

(1) The WKB Approximation of the Fractionation Factor. The double well potential model for the LBHB can be thought of as arising from a combination of two separate harmonic wells. If the vibrational frequency in each well is ω, then the zero-point energy of each well is given by $E_o = \omega/2$. It is well-known that energy states below the barrier in

double well potentials are split by an amount, g. Thus, the set of lowest energies of the double well is given by

$$E_0^{\pm} = \frac{1}{2}\left(\omega \pm \frac{g}{2}\right) \tag{9}$$

where the − sign leads to the lower of the two energies and the + sign the larger. In eq 9, g is the correction due to tunnel splitting. The frequency at the bottom of the well is given by $2\sqrt{B/m}$, with B being the double well potential parameter discussed above. The tunnel splitting factor, g, can be written as

$$g = \frac{\omega}{\pi c^2} \tag{10}$$

where c is given within the WKB approximation as[12]

$$c = \exp\left\{\int_0^{x^*}\left[2m\left(V(x) - \frac{\omega}{2}\right)\right]^{1/2} dx\right\} \tag{11}$$

Here, m is the mass, and $V(x)$ is the potential energy function given in eq 1. The integration limit, x^*, is the inner turning point underneath the barrier at the zero-point energy, $\omega/2$. Our goal is to obtain a simple analytic formula to compute the tunnel splitting, g. The integral in eq 11 can certainly be done numerically for the potential, $V(x)$, given in eq 1. Instead, we use a simple approximation which leads to an integral that can be done analytically. We treat the potential as a parabolic barrier by discarding the quartic, x^4, term, in $V(x)$

$$V(x) \approx D - \frac{B}{2}x^2 \tag{12}$$

The inner turning point for this approximate potential is the $x^* = \sqrt{[1/B](D-\omega/2)}$, and the integral in eq 11 can be performed leading to the final result for c

$$c = \exp\left[\left(\frac{D - \frac{\omega}{2}}{4B}\right)\pi\sqrt{2mB}\right] \tag{13}$$

Now, the final result for tunnel splitting is

$$g = \frac{2\left(\frac{B}{m}\right)^{1/2}}{\pi c^2} \tag{14}$$

If the barrier is large enough, then only the lowest two states in the double well potential contribute to the partition function and the fractionation factor can be computed via

$$\phi_R = \frac{\sum_{\pm} e^{-\beta E_{0,D}^{\pm}}}{\sum_{\pm} e^{-\beta E_{0,H}^{\pm}}} \tag{15}$$

Thus, within the WKB approximation, eqs 9 and 13−15 comprise an analytic expression for the fractionation factor of a LBHB that can be computed on a hand calculator. We will see shortly that the WKB expression for the ϕ_R fails for very small barriers. This is because both of the lowest doublet of eigenstates must be below the barrier for the WKB approach just taken to be valid. If the barrier is too small, then one or both of the lowest eigenstates can be above the barrier and the WKB approximation to the fractionation factor is poor.

(2) The Quantum Corrected Classical Partition Function (QCM). One of us, in a previous work,[13] has shown that the quantum mechanical partition function for a single-dimensional system of mass m can be computed via

$$Q = \left(\frac{m}{2\pi\hbar^2\beta}\right)^{1/2}\int_{-\infty}^{\infty} dx e^{-\beta V(x)} W(x) \tag{16}$$

where V(x) is the potential energy of the system and W(x) is a quantum weighting factor that builds in both zero-point energies and tunneling corrections. The quantum mechanical weight factor is given by

$$W(x) = \frac{\hbar\beta\omega(x)}{2\sinh\left[\hbar\beta\omega(x)/2\right]} \tag{17a}$$

with

$$\omega(x) = \sqrt{\frac{1}{m}\frac{\partial^2 V(x)}{\partial x^2}} \tag{17b}$$

If the second derivative of the potential is negative, then the quantum weight factor takes a different, though similar form, and this is discussed in ref 13. If the potential energy is of N dimensions, then the QCM approximation is readily generalized to

$$Q = \left(\frac{m}{2\pi\hbar^2\beta}\right)^{N/2}\int_{-\infty}^{\infty} d\vec{x} e^{-\beta V(\vec{x})} W(\vec{x}) \tag{18}$$

Now the quantum weight factor is computed from a second-order Taylor expansion of the potential as follows

$$W(\vec{x}) = \prod_j^N \frac{\hbar\beta\sqrt{\lambda_j}(\vec{x})}{2\sinh\left[\hbar\beta\sqrt{\lambda_j}(\vec{x})/2\right]} \tag{19a}$$

where $\lambda_j(x)$is the j^{th} eigenvalue of the mass-weighted force constant matrix, $\underset{\approx}{\mathbf{V}}$

$$[\underset{\approx}{\mathbf{V}}]_{j,k} = \frac{\partial^2 V(\vec{x})}{\partial x_j \partial x_k} \tag{19b}$$

Equations 18 and 19 comprise the working equations for the QCM approximation to the quantum partition function for multidimensional systems. The integral in eq 18 can be done very efficiently via Monte Carlo importance sampling. For the multidimensional model of LBHBs discussed in this work, the quantum weight factor only depends on the proton coordinate and the integration over all other degrees of freedom and can be performed analytically. For the other, two-dimensional, model discussed in this work, we perform the two-dimensional quadrature in eq 18 numerically via the trapezoid rule.

It is useful to think of the QCM partition function as arising from an effective quantum potential energy,[16−19] V_{eff}

$$V_{eff}(\vec{x}) = V_{classical}(\vec{x}) - \left(\frac{1}{\beta}\right)\ln[W(\vec{x})] \tag{20}$$

Here, $V_{\text{classical}}$ is the classical potential. We find that the effective quantum potential defined in eq 20 gives a physically intuitive picture of the effect of other degrees of freedom on the equilibrium properties of the LBHB. The fractionation factor can then be computed within the QCM from the effective quantum potential via

$$\phi_R = \frac{\int d\vec{x} e^{-\beta V_{\text{eff}}^{\text{D}}(\vec{x})}}{\int d\vec{x} e^{-\beta V_{\text{eff}}^{\text{H}}(\vec{x})}} \tag{21}$$

In the above equation, $V_{\text{eff}}^{\text{D}}$ and $V_{\text{eff}}^{\text{H}}$ are effective quantum potentials for deuterium and hydrogen substituted systems, respectively. It is important to point out here that $V_{\text{eff}}^{\text{D}}$ and $V_{\text{eff}}^{\text{H}}$ differ because the weighting factors for each differ due to the different masses, as shown in eqs 17a,b.

(b) Multidimensional Models for LBHBs. Here we discuss two different models that capture effects of other degrees of freedom on the LBHB.

(1) Modulation of Barrier Height. We have found in previous work, that as the donor−acceptor distance is varied in a molecule, the barrier to proton transfer between the sites is modulated.[14] At larger donor−acceptor distances the barrier is higher. This higher barrier indicates a strengthening of the covalent O−H bond and weakening of the hydrogen bond. At smaller donor−acceptor distances the barrier is lower. This indicates the strengthening of the hydrogen bond and weakening of the covalent bond.

At nonzero temperature it is reasonable to assume that many intramolecular modes of motion will couple to the proton coordinate and modulate the donor−acceptor distance, and thus, the barrier. Here we couple the proton coordinate x to a vibrational mode, y, that measures the distance between the donor and acceptor sites. The potential for this model is given by

$$V(x,y) = A(y)x^4 - B(y)x^2 + \frac{B(y)^2}{4A(y)} + \frac{\mu\omega^2}{2}y^2 \tag{22}$$

where μ and ω are mass and frequency of y degree of freedom. Now the coefficients A and B depend explicitly on coordinate y via

$$A(y) = A_o e^{-\alpha y} \tag{23a}$$

$$B(y) = B_o e^{\alpha y} \tag{23b}$$

Here, α is a parameter that couples the intramolecular vibrational coordinate, y, to the LBHB coordinate, x. As shown by eq 2, the barrier is given by $B^2/4A$. Thus, as donor−acceptor distance increases (larger y), A decreases and B increases according to eq 23. Therefore, the barrier increases for large values of y. It is also easy to see that eq 23 lead to a decreasing barrier height with decreasing donor−acceptor distance, y.

(2) LBHB Coupled to External Solvent. A well accepted and widely used model of solvent effects on a chemical system is the Generalized Langevin equation (GLE). The classical form of the GLE is given by[20]

$$\mu\ddot{x}(t) = -\frac{\partial V(x)}{\partial x} - \int_o^t ds\eta(t-s)\dot{x}(s) + F(t) \tag{24}$$

where $\eta(t)$ is the so-called friction kernel and $F(t)$ is a randomly fluctuating force.

It is well-known that the GLE is isomorphic to a system coordinate, x, coupled to a set of N harmonic oscillators, $\{\vec{y}\}$.[21] The potential energy for this mapping with our potential for proton coordinate, x, is given by

$$V(x,\vec{y}) = Ax^4 - Bx^2 + \frac{\mu}{2}\sum_j^N \omega_j^2(y_j - c_j x)^2 \tag{25}$$

The frequencies and couplings of this harmonic bath can be computed from[22]

$$\omega_j = \frac{\pi}{\tau}\left(j - \frac{1}{2}\right) \quad j = 1,2,...N \tag{26a}$$

$$c_j^2 = \frac{2f\sigma^2}{\mu\tau}\frac{e^{-[(\omega_j\sigma)^2]/2}}{(\omega_j\sigma)^2} \tag{26b}$$

Here, f is the friction strength, and σ and τ set the timescale of the friction. In all calculations in this work we choose $\tau = 2\sigma$.

Within this model, the partition function can be computed very efficiently by using the QCM. The force constant matrix is completely independent of the oscillator coordinates, $\{\vec{y}\}$, and the matrix elements are

$$[\underset{\approx}{V}]_{11} = \frac{\partial^2 V}{\partial x^2} = 12Ax^2 - 2B + \sum_j^N \mu\omega_j^2 c_j^2 \tag{27a}$$

$$[\underset{\approx}{V}]_{1j} = \frac{\partial^2 V}{\partial x \partial y_j} = -\mu\omega_j^2 c_j^2 \tag{27b}$$

$$[\underset{\approx}{V}]_{kk} = \frac{\partial^2 V}{\partial y_k^2} = -\mu\omega_k^2 \quad \text{for k} > 1 \tag{27c}$$

Since the force constant matrix is independent of $\{\vec{y}\}$, the integration over all oscillators can be performed analytically yielding

$$Q = \prod_{j=1}\left(\frac{1}{\beta\omega_j}\right)\int dx e^{-\beta(Ax^4 - Bx^2)}W(x) \tag{28}$$

At each value of x we diagonalize the force constant matrix given in eq 27. The weight is then computed from the square root of all the eigenvalues via

$$W(x) = \prod_{j=1}^{N+1}\frac{\beta\hbar\sqrt{\lambda_j(x)}}{2\sinh\left(\frac{\beta\hbar\sqrt{\lambda_j(x)}}{2}\right)} \tag{29}$$

where $\lambda_j(x)$ is the j$^{\text{th}}$ eigenvalue of the force constant matrix at point x.

It should be noted that the special form of the coupling between solvent and the LBHB makes the computation of the partition function very computationally efficient. If the coupling between the solvent was anharmonic the integral needed to compute the partition function in eq 21 can be

Table 1. Comparison of (a) Partition Functions and (b) Fractionation Factors Computed from the Exact, WKB, and QCM Methods

(a) Partition Functions

A (a.u)	B (a.u)	barrier height (kJ mol^{-1})	partition functions		
			exact	QCM	WKB
0.10	0.15	147.66	1.72×10^{-4}	1.80×10^{-4}	1.42×10^{-4}
0.10	0.10	65.63	1.12×10^{-3}	1.19×10^{-3}	8.20×10^{-4}
0.10	0.05	16.41	1.94×10^{-2}	1.97×10^{-2}	1.39×10^{-2}
0.10	0.025	4.10	0.12	0.12	1.80

(b) Fractionation Factors

A (a.u)	B (a.u)	barrier height (kJ mol^{-1})	fractionation factors		
			exact	QCM	WKB
0.10	0.15	147.66	14.83	12.89	16.41
0.10	0.10	65.63	8.33	8.10	9.82
0.10	0.05	16.41	3.04	3.08	3.02
0.10	0.025	4.10	1.92	1.83	0.31

computed via importance sampling. We expect such a sampling technique would make moderately sized systems (on the order of 10−100) degrees of freedom amenable to calculation.

III. NUMERICAL RESULTS

(a) Comparison of WKB, QCM, and Exact Partition Functions and Fractionation Factors for a One-Dimensional System. The eigenenergies can be computed exactly for a single-dimensional system and thus also the partition functions and fractionation factors. We solve the Schrodinger equation exactly for the double well potential given in eq 1. The wave function in expanded in a basis set of particle in a box eigenfunctions. We find that a box length of $l = 4$ A and 50 particle in a box basis functions suffices for results to converge. The partition functions are then computed from the Boltzmann sum over the eigenenergies.

In Table 1 (a) we compare exact, QCM, and WKB results for the partition function of double well potentials with barrier heights ranging from high (∼150 kJ mol^{-1}) to low (∼4 kJ mol^{-1}). For reference, a typical LBHB has a barrier < 20 kJ mol^{-1}. It is seen from Table 1(a) that the QCM results compare very favorably to exact results over the whole range of barrier heights. The WKB results, by contrast, are not nearly as accurate as the QCM results and compare quite unfavorably at low barrier heights.

In Table 1(b) we compare exact, QCM, and WKB results for the fractionation factor as defined in eq 8. We compute these fractionation factors by computing partition functions for protonated and deuterated double well potentials and taking their ratio. We find, again, that the QCM results compare more favorably to the exact results than the WKB. The reason the WKB results fail so miserably at low barrier heights is because at low barrier heights all eigenstates are *above* the barrier in energy and the WKB approximation taken in this work is no longer valid. For example, at the low barrier height of 4.1 kJ mol^{-1}, the energy of the lowest eigenstate is 5.5 kJ mol^{-1}, i.e., well above the barrier. It is interesting to note that the WKB results for the fractionation factors are not too bad, except for the lowest barrier height studied.

As mentioned previously, the one advantage of the WKB approach is that it leads to an analytical expression for the fractionation factor. This is useful for the following reason. If the experimental value of the fractionation factor is known *and* one other measure of the LBHB is known, then it is possible to determine the barrier height, D, and curvature at the bottom of the well from eqs 13−15. For example, if the distance between donor and acceptor sites is known from an X-ray diffraction measurement, then the relation between this distance, Δx, and the A and B parameters is

$$\Delta x^2 = \frac{2B}{A} \tag{30}$$

Thus, one of the parameters, *B*, for example, can be expressed in terms of *A*, and the known donor−acceptor distance, Δx. Equation 13 then only depends on *A*. The value of *A* can then be computed from the value of the fractionation factor, and *B* can be determined from eq 30. Once *A* and *B* are known, the barrier height and curvature can be estimated.

Table 2. Fractionation Factors for the Two-Dimensional LB HB System as a Function of Coupling Strength as Discussed in the Text

α ($\times 10^{-9}$ m^{-1})	ω (cm^{-1})	ϕ_R
1.0	250	3.01
3.0	250	2.68
5.0	250	2.33
1.0	500	3.06
3.0	500	2.97
5.0	500	2.79

(b) Two Models for Multidimensional Systems Containing a LBHB. (1) Coupling of the LBHB to an Intramolecular Vibration. We now use the QCM to approximate the effect of an intramolecular vibration that modulates the donor−acceptor distance and the barrier height. We use the two-dimensional potential defined by eqs 22 and 23. The partition functions of protonated and deuterated LBHBs are computed using eqs 18 and 19. The two-dimensional integral in eq 18 is performed by the trapezoid rule. At each (x,y) point the force constant matrix is computed via eq 19b and is diagonalized. The two eigenvalues are computed, and the quantum weight function is computed via eq 19a. We present results of this system in Table 2. We compute fractionation factors for increasing coupling values of α in eqs 23. When $\alpha = 0$, the coupling between the LBHB and y-coordinate is turned off. As α is increased, the effect of the y-coordinate on the LBHB is turned on.

The first three rows of Table 2 show the fractionation factors for values of $\alpha = 1.0 \times 10^9$ m^{-1}, 3.0×10^9 m^{-1}, and 5.0×10^9 m^{-1}, when the frequency of the donor−acceptor vibration is $\omega = 250$ cm^{-1}. The values of A and B are 0.1 au and 0.05 au, respectively. The table shows that as the coupling is turned up, the fractionation factor decreases. It decreases by as much as a third for the largest coupling studied. This is a large decrease in the fractionation factor in view of the fact that an experimentalist will consider a value of $\phi = 1$ a high barrier hydrogen bond and a value of $\phi_R = 0.75$ a LBHB.

The last three rows of Table 2 show the fractionation factor values for values of $\alpha = 1.0 \times 10^9$ m^{-1}, 3.0×10^9 m^{-1}, and 5.0×10^9 m^{-1} for a larger value of the donor−acceptor vibrational frequency, i.e., $\omega = 500$ cm^{-1}. The values of A and B are 0.1 au and 0.05 au, respectively. We see that the fractionation factors decrease as the coupling is turned up.

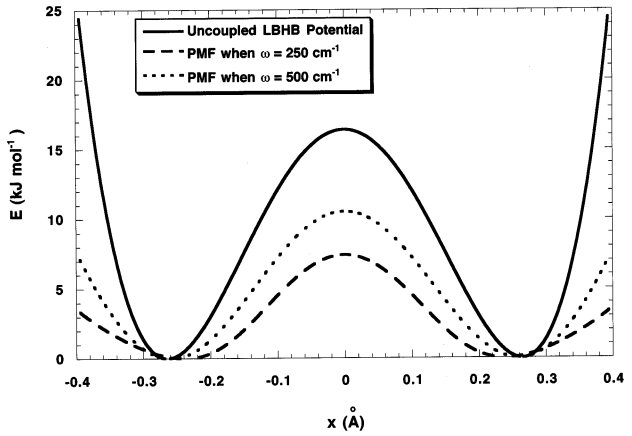

Figure 2. The PMFs for the barrier modulation model. The solid line shows the uncoupled potential along the hydrogen bond coordinate. The long dashed line shows the PMF along the hydrogen bond coordinate when $\alpha = 5.0 \times 10^9$ m^{-1} and the donor−acceptor vibrational frequency is 250 cm^{-1}. The short dashed line shows the PMF when $\alpha = 5.0 \times 10^9$ m^{-1} and the donor−acceptor vibrational frequency is 500 cm^{-1}.

There is less of a decrease in the fractionation factor values for the larger vibrational frequency. This is because at T = 300 K, the RMS displacement between the donor and acceptor is smaller for the vibration with the larger frequency.

The decrease in the value of the fractionation factor is due to the coupling of the LBHB coordinate to the intramolecular coordinate, y, which modulates donor and acceptor distance. The effect of this coordinate is to lower the effective potential barrier felt by the x (LBHB) coordinate. To demonstrate this effect we show the potential of mean force (PMF) felt by the x-coordinate due to the coupling to the y-coordinate. The PMF is the potential felt by the LBHB averaged over the y-coordinate, i.e.

$$e^{-\beta w_{PMF}(x)} = \int dy e^{-\beta V(x,y)} \tag{31}$$

Here, $w_{PMF}(x)$ is the PMF along the LBHB coordinate and $V(x,y)$ is the full two-dimensional potential in eq 22.

In Figure 2 we show the PMFs for an α coupling value of $\alpha = 5.0 \times 10^9$ m^{-1} for $\omega = 250$ cm^{-1} (the long dashed line) and $\omega = 500$ cm^{-1} (the short dashed line). As shown by Figure 2, the PMF show smaller barriers than the uncoupled LBHB potential (solid line). As demonstrated above, lower barriers mean stronger hydrogen bonds and lower values of the fractionation factor. Further, the PMF for the lower frequency intramolecular vibration, $\omega = 250$ cm^{-1}, shows a lower barrier than the PMF for the larger frequency, $\omega = 500$ cm^{-1}, vibration. This is why the fractionation factors are lower for the lower frequency vibration coupling at a given value of α.

(2) Coupling of the LBHB to External Solvent Modes. We now use the QCM to approximate the effects of solvent degrees of freedom on the fractionation factors of LBHBs. We consider solvents of two different time scales of friction, a slow response regime with $\sigma = 300$ fs, and a fast response regime with $\sigma = 800$ fs. We vary the friction strength, f, of each bath from zero to $f = 2 \times 10^{-4}$. We have found that baths containing 10 oscillators [a value of N in eq 26] are large enough to converge all results.

The first three rows of Table 3 show the values of the fractionation factors when the solvent is in the slow response regime, i.e., $\sigma = 300$ fs, and the friction strength, f (in a.u.), is 0.5×10^{-4}, 1.0×10^{-4}, and 2.0×10^{-4}. The values for A and B are 0.07 au and 0.04 au, respectively. These values of A and B lead to a LBHB of barrier height of 15 kJ mol^{-1}. It is apparent that as the friction strength increases, the fractionation factor decreases. The last three rows of Table 3 show the same phenomenon of decreasing fractionation factors with an increase in the friction strength, this time with a faster responding solvent with $\sigma = 800$ fs. For all values of the friction strength, f, the fractionation factors are lower for the slower responding solvent, indicating an apparent strengthening of the hydrogen in the slower solvent compared to the faster solvent.

The mechanism by which the fractionation factors are lowered by solvent coupling is quite different from the mechanism due to barrier height modulation discussed above.

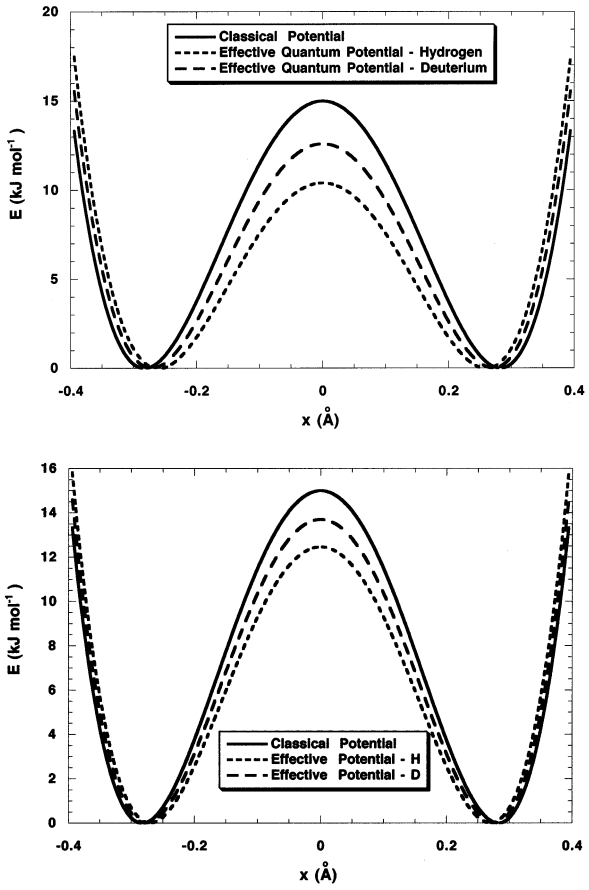

Figure 3. The effective quantum mechanical potentials along the hydrogen bond coordinate for the solvent coupling model. In all panels the solid line is the classical potential, the short dashed line is the effective quantum potential for hydrogen, and the long dashed line is the effective quantum potential for deuterium. In panel (a) the value of the friction is $f = 0.5 \times 10^{-4}$ a.u., and in panel (b) the value of the friction strength is $f = 2.0 \times 10^{-4}$ a.u.

Table 3. Fractionation Factors for the LBHB in the Presence of Solvent at Various Friction Strengths and Time Scales

σ (fs)	f (a.u.)	ϕ_R
300	0.5×10^4	2.21
300	1×10^{-4}	2.04
300	2×10^{-4}	1.88
800	0.5×10^{-4}	2.40
800	1×10^{-4}	2.26
800	2×10^{-4}	2.09

The PMF along the LBHB coordinate defined in eq 31, when computed for the potential given by eq 25, is identical to the original potential along this coordinate.[26] In other words, the average potential felt by the proton (or deuteron) is unaffected by the averaging over bath coordinates, $\{\vec{y}\}$. The lowering of the fractionation factor, in the case of coupling to solvent, is a completely quantum mechanical effect. We show this by computing the effective quantum potential given in eq 20. The effective quantum potential for H and D for friction strength of $f = 0.5 \times 10^{-4}$ and $\sigma = 300$ fs is shown in Figure (3a) by the short and long dashed line, respectively. The effective quantum potential for H and D for friction strength of $f = 2.0 \times 10^{-4}$ and $\sigma = 300$ fs is shown by the short and long dashed line in Figure 3b, respectively. As shown by the figures the solvent has the effect of making the effective quantum potential look more like the initial classical potential. Classically, the reduced fractionation factor attains a value of $\sqrt{2}$. As the friction strength is turned up the coupling of the LBHB to the solvent is increased and the classical and effective quantum potentials become more similar. Thus, as the friction strength is turned up, the fractionation factor approaches the value of $\sqrt{2}$.

IV. CONCLUSION

Our goal in this work has been 2-fold. First, to test the accuracy of two approximation methods for computing fractionation factors of LBHBs. The first approximation presented was the WKB approximation. We found that this approximation is of limited accuracy and that it fails completely when the lowest eigenstate is above the barrier. We also pointed out that the WKB approximation presented here is limited to isolated, single-dimensional LBHBs. The one advantage of the WKB approximation was that it led to an analytical expression for the fractionation factor. We further showed that the resulting WKB equation for the fractionation factor can be used to determine barrier height and well curvature if another experimental datum on the LBHB is known.

The other approximation method presented here is the QCM that corrects the classical partition function by a simple quantum correction term. This approximation has been derived and presented in previous work, but here we show that it is very efficient and accurate for computing fractionation factors of LBHBs. Further, we show that this approximation generalizes quite easily to treat LBHBs that are coupled to other degrees of freedom.

The second goal of this work was to critically assess two different, but physically relevant, models of effects of other degrees of freedom on the LBHB. These other degrees of freedom were either intramolecular, i.e., an intramolecular vibration, or external to the molecule such as surrounding solvent. The two models presented here show that coupling of a LBHB to intra- or external molecular modes lowers the fractionation factor. This is an important result because it points to the possibility of misinterpretation of the fractionation factor value. Lower values of the fractionation factor do not necessarily mean the intrinsic hydrogen bond barrier is small. It means, in the presence of all other degrees of freedom in the system, the hydrogen bond is stronger and the barrier is smaller.

We have shown that the mechanism for the lowering of the LBHB fractionation factor is different for coupling to intramolecular degrees of freedom than from coupling to external degrees of freedom. We saw that for the potential that models the modulation of the barrier height due to an intramolecular vibration, the fractionation factor is lowered because the effect of averaging over the vibrational coordinate is to lower the barrier. The lowering of the barrier leads to lower fractionation factors. For coupling to external solvent, the fractionation factor is lowered because the effective quantum mechanical potential felt by the hydrogen bond coordinate becomes closer to the classical potential as the solvent coupling is turned up. This also leads to a lowering of the fractionation factor.

ACKNOWLEDGMENT

M. Messina would like to acknowledge the support from the donors of the Petroleum Research Fund, administered by the ACS.

REFERENCES AND NOTES

(1) Cleland, W. W.; Kreevoy, M. M. Low-barrier hydrogen bonds and enzymic catalysis. *Science* **1994**, *264*, 1887−1890.
(2) Guthrie, J. P. Short strong hydrogen bonds: can they explain enzymic catalysis? *Chem. Biol.* **1996**, *3*, 163−170.
(3) Lin, J.; Westler, W. M.; Cleland, W. W.; Markley, J. L.; Frey, P. A. Fractionation factors and activation energies for exchange of the low barrier hydrogen bonding proton in peptidyl trifluoromethyl ketone complexex of chymotrypsin. *Biochemistry* **1998**, *95*, 14664−14668.
(4) Frey, P. A.; Whitt, S. A.; Tobin, J. B. A low-barrier hydrogen bond in the catalytic triad of serine proteases. *Science* **1994**, *264*, 1927−1930.
(5) Neidhart, D.; Wei, Y.; Cassidy, C.; Lin, J.; Cleland, W. W.; Frey, P. A. Correlation of low-barrier hydrogen bonding and oxyanion binding in transition state analogue complexes of chymotrypsin. *Biochemistry* **2000**, *40*, 2439−2447.
(6) Shan, S.; Herschlag, D. The change in hydrogen bond strength accompanying charge rearrangement. Implications for enzymic catalysis. *Proc. Natl. Acad. Sci. U.S.A.* **1996**, *93*, 14474−14479.
(7) Mangel, W. F., et. al.; Sweet, R. M. Structure of an acyl-enzyme intermediate during catalysis: (guanidinobenzoyl) trypsin. *Biochemistry* **1991**, *29*, 8351−8357.
(8) Xiang, S.; Short, S. A.; Wolfenden, R.; Carter, C. W. Transition-state selectivity for a single hydroxyl group during catalysis by cytidine deaminase. *Biochemistry* **1995**, *34*, 4516−4523.
(9) Carlow, D. C.; Smith, A. A.; Yang, C. C.; Short, S. A.; Wolfenden, R. Major contribution of a carboxymethyl group to transition-state stabilization by cytidine deaminase: mutation and rescue. *Biochemistry* **1995**, *34*, 4220−4224.
(10) Cassidy, C.; Lin, J.; Frey, P. A. A new concept for the mechanism of action of chymotrypsin: the role of the low barrier hydrogen bond. *Biochemistry* **1997**, *36*, 4576−4584.
(11) Kreevoy, M. M.; Liang, T. M. Structures and isotopic fractionation factors of complexes, $A_1HA_2^-$. *J. Am. Chem. Soc.* **1980**, *102*, 3315−3322.
(12) Bohm, D. *Quantum Theory*; Prentice-Hall: New York, U.S.A., 1951; p 265
(13) Messina, M.; Schenter, G. K.; Garrett, B. C. Approximate path integral methods for partition functions. *J. Chem. Phys.* **1993**, *98*, 4120−4127.
(14) Ventura, K. M.; Greene, S. N.; Halkides, C. J.; Messina, M. A mixed quantum-classical approach for computing effects of intramolecular motion on the low-barrier hydrogen bond. *Struct. Chem.* **2001**, *12*, 23.
(15) McQuarrie, D. A. *Statistical Mechanics;* Harper & Row: New York, U.S.A., 1976; pp 142−159.
(16) Voth, G. A. On the use of Feynman-Hibbs effective potentials to calculate quantum mechanical free energies of activation. *J. Chem. Phys.* **1991**, *94*, 4095.
(17) Valone, S. M.; Voter, A. F.; Doll, J. D. The isotope and temperature dependence of self-diffusion for hydrogen, deuterium and tritium on Cu(100) in the 100−1000 K range. *Surf. Sci.* **1985**, *155*, 687.
(18) Valone, S. M.; Voter, A. F.; Doll, J. D. The influence of substrate motion on the self-diffusion of hydrogen and its isotopes on the Cu-(100) surface. *J. Chem. Phys.* **1986**, *71*, 7480.

(19) Doll, J. D.; Myers, L. E. Semiclassical Monte Carlo methods. *J. Chem. Phys.* **1979**, *71*, 2880.
(20) For an inclusive set of references, see: Hangii, P.; Talkner, P.; Borkovec, M. Reaction-rate theory: fifty years after Kramers. *Rev. Mod. Phys. 62*, 251.
(21) Zwanzig, R. Nonlinear generalized Langevin equations. *J. Stat. Phys.* **1973**, *9*, 215.
(22) McRae, R. P.; Schenter, G. K.; Garrett, B. C.; Haynes, G. R.; Voth, G. A.; Schatz, G. C. Critical comparison of approximate and accurate quantum mechanical calculations of rate constants for a model activated reaction in solution. *J. Chem. Phys. 97*, 7392.

CI0202943